

Development and Application of a Novel Calorimetry Technique for the Study of Lithium-Ion Cell Thermal Runaway

Steven L. Rickman¹

NASA Engineering and Safety Center, Houston, TX, 77058

Lithium-ion battery technology is widely used and is attractive due to demonstrated specific energies in the 200-300 W-hr/kg range. The excellent, mass-efficient energy storage capability of lithium-ion batteries has led to their use on many aerospace platforms. However, lithium-ion batteries can exhibit thermal runaway behavior wherein stored electrochemical energy is released rapidly as a result of thermal or mechanical failure, electrochemical abuse, internal or external short circuiting. A single cell undergoing thermal runaway within a battery has the potential to induce thermal runaway in adjacent cells if heat dissipation is not properly managed and can result in a catastrophic failure of the battery. Designing batteries that are resistant to thermal runaway propagation requires an understanding of, not only, total energy yield but also the means by which that energy is liberated from the cell. While Accelerating Rate Calorimetry and other techniques provide total thermal runaway energy yield, they do not provide the fractional breakdown of energy liberated via conduction through the cell casing from that which is vented from the cell as hot gases and effluents. Such data are needed to inform battery thermal design and analysis. To measure the total energy yield, the fraction conducted through the cell casing, and the fraction lost due to gases and effluents, NASA developed Fractional Thermal Runaway Calorimetry (FTRC). Two calorimeters have been developed and demonstrated, the Small-format- and Large-format-Fractional Thermal Runaway Calorimeters (S-FTRC and L-FTRC, respectively). The technique has been successfully applied to small- and large-format cells (2.4-3.5 Ah and >100 Ah capacity, respectively) and has given new insights into Li-ion cell thermal runaway. Development of the calorimeters is discussed and results from the initial thermal runaway testing campaigns are presented.

Nomenclature

ARC	= accelerating rate calorimetry
BV	= bottom vent
c_{p_i}	= specific heat of calorimeter subcomponent i (which can vary with temperature)
EVA	= extravehicular activity
FTRC	= Fractional Thermal Runaway Calorimetry
L-FTRC	= Large-format – Fractional Thermal Runaway Calorimeter
LREBA	= Lithium-ion Rechargeable EVA Battery Assembly
m_i	= mass of calorimeter subcomponent i
NBV	= non-bottom vent
n	= number of instrumented calorimeter subcomponents
Q_i	= heat gained in calorimeter subcomponent i due to change in temperature
Q_{total}	= total thermal runaway energy yield
SEI	= solid electrolyte interphase
S-FTRC	= Small-format – Fractional Thermal Runaway Calorimeter
ΔT_i	= temperature change in calorimeter subcomponent i

¹ NASA Technical Fellow for Thermal Control and Protection, NASA Engineering and Safety Center, 2101 NASA Parkway, Mail Stop: WE, Houston, TX 77058.

I. Introduction

LITHIUM-ION (Li-ion) battery technology has demonstrated specific energies in the range of 200-300 W-hr/kg¹. For spacecraft, providing high energy and power with as little mass as possible is desirable given the cost of launching or landing mass. These strengths are also attractive for many terrestrial applications. Even though Li-ion cells have advantages from a specific energy and specific power perspective, they have a downside that cannot be neglected. As has been widely reported in the media, there are many instances whereby Li-ion cells have undergone a rapid exothermic decomposition and subsequent release of their stored energy²⁻⁴. This is referred to as thermal runaway and can arise as a result of thermal failure due to overheating, mechanical failure such as a nail puncture, electrochemical abuse due to charging/discharging, and internal or external short circuiting. Often, cells are arranged into a battery where cells are packed into close proximity to produce a mass- and volume-efficient configuration. In addition to the possibility of a single cell within a battery going into thermal runaway, designs must also consider the propensity of that thermal runaway to propagate to adjacent cells within the battery which could have serious and potentially catastrophic system impacts.

There are a number of exothermic processes that contribute to thermal runaway including electrolyte breakdown, anode and solid electrolyte interphase (SEI) decomposition, cathode decomposition and oxygen release, electrolyte oxidation, and oxidation of the electrolyte in the surrounding air if an atmosphere is present⁵. While these reactions do not include the involvement of plastics within the battery, the oxidation of these plastics is estimated to be as great as the contribution of the electrolyte in terms of heat release, on the order of 2.5 MJ for plastics versus 1.92 MJ for electrolyte per kilogram of battery⁶. Therefore, it is important to understand that the energy yield from thermal runaway has the potential to be more than the amount of electrical energy stored in the cell.

II. Early Work

In response to the 2013 Boeing 787 Dreamliner incident⁷, NASA placed additional emphasis on Li-ion battery safety by assuming a thermal runaway will eventually happen. Any new design should ensure that such a thermal runaway event is not catastrophic and should demonstrate that propagation to surrounding cells would not occur⁸.

In 2014, NASA pursued thermal modeling of the Lithium-ion Rechargeable Extravehicular Activity (EVA) Battery Assembly (LREBA) to inform design decisions and understand the results of extensive development testing with the goal of enhancing safety against the possibility of thermal runaway propagation. A complete representation of heat transfer mechanisms required a quantification of heat transfer through the cell casing as well as heat transferred from the cell via vented gases and effluents resulting from thermal runaway. Single cell models representing reaction rates and isentropic flow equations during venting were used for preliminary estimates of thermal runaway energy yield. A model developed using methodology from Hatchard, et al.⁹ was used to establish an early estimate of the energy liberated during a thermal runaway event. The heating profile resulting from this internal model was used to develop a simplified, homogeneous cell thermal model where logic within the model was used to trigger the thermal runaway when any node reached a specified thermal runaway onset temperature. While this model was successful in modeling some gross characteristics of the thermal response, it did not allow representation of the heat soak to the cell casing from the internal cell winding¹⁰.

A more detailed cell model (Figure 1) was pursued but given that direct internal cell temperature measurement was not possible, the value of the model could only be assessed based on externally observable events and post-test evidence such as: matching cell pre-heating rate and time to trigger thermal runaway as compared to testing, measurement of cell casing peak temperature, and post-test destructive physical analysis to determine whether aluminum and copper within the cell had melted¹⁰. But in order to achieve correlation, the total energy yield from the thermal runaway event and how it was escaping from cell were needed. While total energy estimates could be obtained from the multi-physics model, the test-to-test variability was not known. And while testing techniques such as accelerating rate calorimetry could provide total energy yield and test-to-test variability, the energy fraction conducted through the cell casing versus the fraction released as hot gases and effluents could not be readily determined.

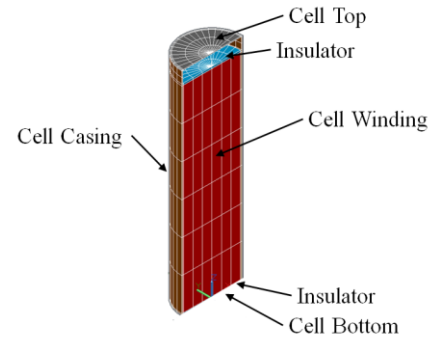


Figure 1. Cross-sectional view of detailed 18650 Li-ion cell thermal network model.

The model was used for an analytical comparison with a thermal runaway test of an array of 18650 cells in a “picket fence” arrangement as shown in Figure 2a-c. A single cell was triggered into thermal runaway which heated an adjacent cell until it was triggered into thermal runaway. Propagation continued until all nine cells experienced thermal runaway. An analytical model using the previously mentioned cell model showed the same propagation behavior as shown in Figure 2d-f¹⁰. However, the model suggested the thermal runaway behavior propagated faster than was observed during test. While the test showed that considerable energy was being lost due to the release of cell contents, the model assumed heat loss via conduction through the cell casing only. Such an assumption could lead to propagation in the thermal model faster than was observed in test. Clearly, all data needed to build an accurate model were not available.

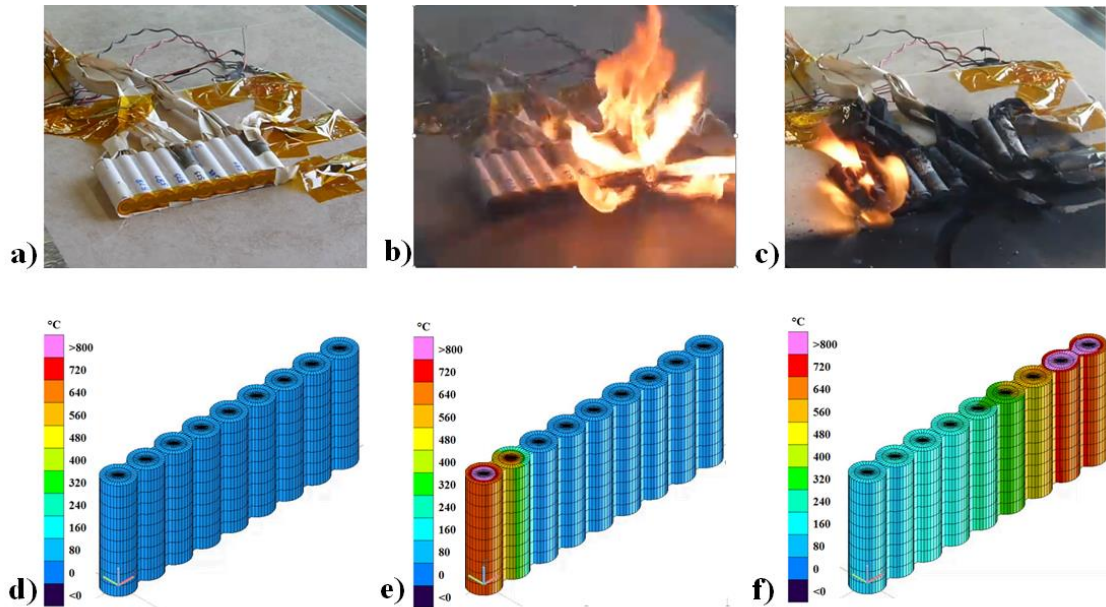


Figure 2. Comparison of 9P “picket fence” 18650 test with thermal analysis showing the propagation of thermal runaway to all cells.

III. Motivation for a New Type of Calorimeter

To obtain the required data, a number of different calorimetry techniques were investigated including accelerating rate calorimetry (ARC), bomb calorimetry, and copper slug calorimetry. ARC is used to determine the onset of self-

heating and thermal runaway in cells. Cells undergoing ARC are heated slowly, using a heat-wait-see methodology, which can result in cell venting considerably prior to the onset of thermal runaway and may not be representative of field failures that might occur as a result of nail penetration or triggering methods. Furthermore, a test can take days and is not practical if a larger number of tests are to be performed to gather statistical data. A tally of the total thermal energy yield is available¹¹. Bomb calorimetry may also be used to measure total energy yield. Copper slug calorimetry can provide data on the rate of mass ejection during thermal runaway but must be used in conjunction with bomb calorimetry to tally the energy yield. None of the surveyed techniques can discern the fractions of energy that conduct through the cell casing, and that which is liberated in the winding, vent gases, and ejecta from the total energy yield⁸. If such data are needed, a new technique is required.

With the previously mentioned shortcomings of the LREBA analysis and the calorimetry techniques available, an effort to develop a new calorimetry technique was pursued for the widely used 18650-size cell. To be of greatest utility, any new technique must provide⁸:

- quantification of total thermal runaway energy yield
- separate tallies of thermal runaway energy conducting through the cell casing, energy contained in the cell winding, and energy liberated as vented gases and effluents
- the ability to measure the volume of liberated gases
- the ability to collect vent gases for subsequent compositional analyses
- the ability to rapidly test cells enabling the collection of statistically significant quantities of data.

A. Small-format – Fractional Thermal Runaway Calorimeter (S-FTRC)

With the dearth of data required to inform battery design and thermal analysis, an effort to develop a new technique, dubbed Fractional Thermal Runaway Calorimetry (FTRC) was initiated in 2016. Given the ubiquity of the popular 18650-sized cell, initial focus was given to the development of a calorimeter capable of measuring thermal runaway energy yield and fractions for these cells which are in the 2.4-3.5 Ah range. The S-FTRC design evolved over seven iterations during the study and was later patented¹² with continued improvements made thereafter. An overview of the S-FTRC configuration with the upper insulated lid removed is shown in Figure 3.

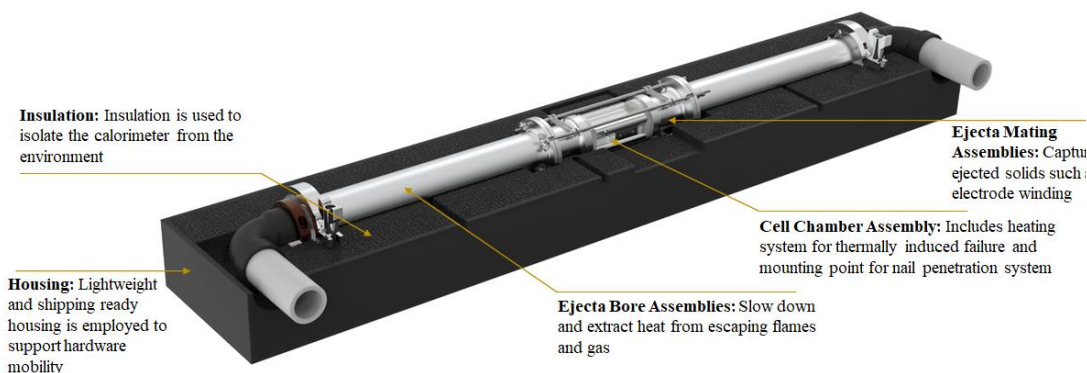


Figure 3. Overview of the Small-format – Fractional Thermal Runaway Calorimeter (S-FTRC) with upper insulated lid removed. (Adapted from Ref. 8)

S-FTRC was designed to accommodate different cell types including those with both, top and bottom vents. Initial designs focused on cylindrical format cells while later versions provided accommodation for pouch format cells. The calorimeter is shown in the “ambidextrous” configuration in Figure 4. The entire calorimeter is housed in an insulated case to limit heat loss to the environment. At the heart of the calorimeter is the cell chamber. This region is thermally isolated from the remainder of the upstream and downstream calorimeter components so that when a cell placed into the chamber is set into thermal runaway, the heat conducting through the casing can be measured separately. High flux heaters force the cell into thermal runaway quickly which is more representative of field failures. Adjacent to the

cell chamber is the ejecta mating assembly which is designed to capture a cell winding (or jellyroll) if ejected during the runaway event. Further downstream, hot gases and effluents venting from the cell pass through a series of baffles configured to produce a tortuous flow path. Particulates from the flow are deposited onto the baffles and heat is absorbed before passing through a copper mesh where additional particulates and heat are removed. The calorimeter is instrumented with an array of thermocouples on key components where temperature measurements are recorded during the thermal runaway. The S-FTRC supports quick turnaround allowing many tests in a day. Rapid data collection and turnaround are key features and allow acquisition of statistically significant quantities of data.

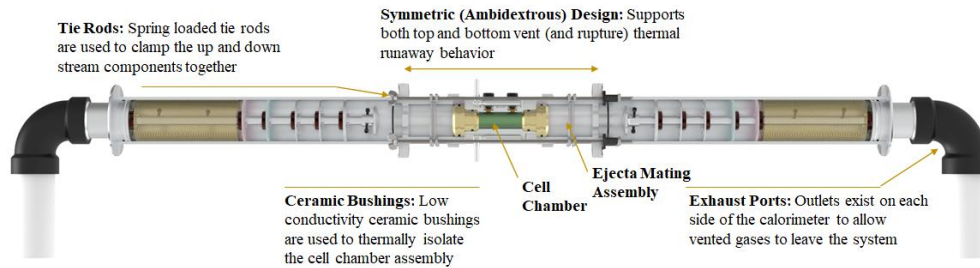


Figure 4. S-FTRC shown in the ambidextrous configuration with cell placement at center. (Adapted from Ref. 8)

The internal configuration is shown in Figure 5. During a typical test, heat is applied to the cell in the cell chamber. Temperature and pressure within the cell rise until the cell vent is breached releasing hot gases and effluents into a pipe and through a series of baffles.

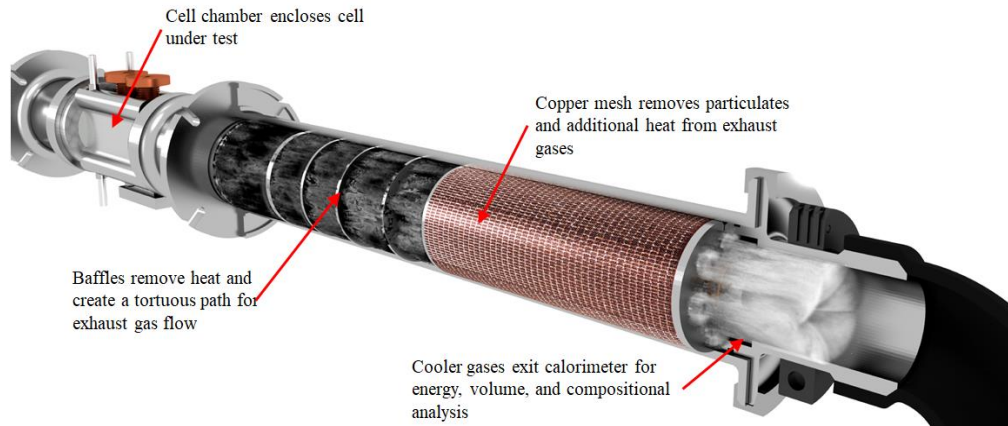


Figure 5. S-FTRC internal configuration detail depicting the flow of hot gases and particulates. (Adapted from Ref. 8)

Total thermal runaway energy yield is tallied using a custom Energy Yield Algorithm (EYA) by summing the energy increase of calorimeter components with known masses and specific heats⁸ using the measured temperature rise for each component, as measured with the previously described array of thermocouples, as shown in Eq. 1.

$$Q_{total} = \sum_{i=1}^n Q_i = \sum_{i=1}^n m_i c_p \Delta T_i \quad (1)$$

The specific heat (c_p) of a given calorimeter component may vary with temperature, which is also accounted for by the EYA. The mass contribution of soot deposited throughout the system is also considered in energy tally calculations. System energy loss was measured during calibration and is accounted for in final energy yield estimates.

In addition to the total thermal runaway energy yield, the calorimeter separates the fraction of that energy released through the cell casing from the fraction that leaves the cell via vented effluents and gases. Since no two thermal runaway events are identical, it is important to gain insight into the range of possible energy yields and their distributions. These variations can be due to random and non-random factors. From the data and the post-processing, distributions are obtained and can be used to formulate a regression model to predict energy release.

Results from an early 18650 testing campaign using a number of cell types are shown in Figure 6¹³. To design a battery that is robust against thermal runaway propagation, data like those presented here are critical to understanding the range of energy yields for thermal runaway events. As is evident in the plot, some cells tend to show a wider range of possible outcomes whereas some have a narrower range of responses. The range of possibilities must be understood as the thermal runaway energy yield for a particular type of cell is not a single number.

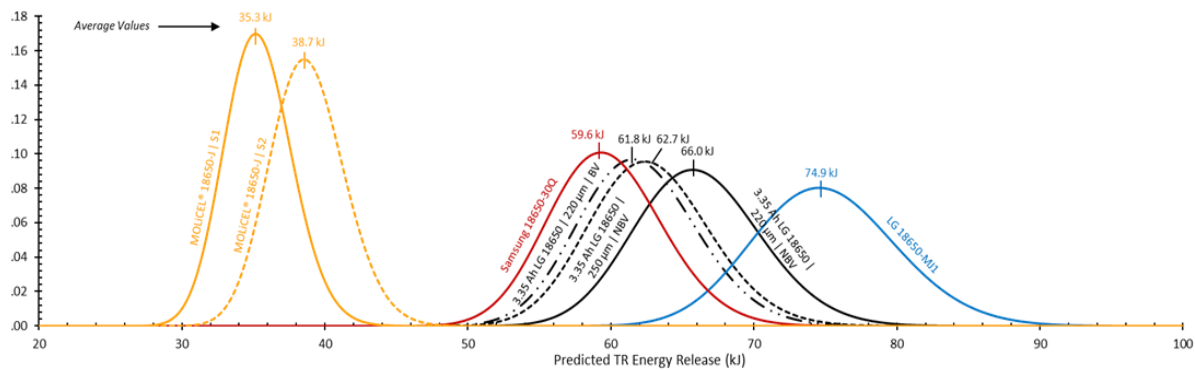


Figure 6. Distribution of total thermal runaway energy yields derived from S-FTRC test data depicting the relative energy yields and expected ranges of cells tested with bottom vents (BV) and without (NBV).

In addition to rapid test capability and total energy yield, a key advantage of fractional thermal runaway calorimetry is that it provides insight into *where* the energy is going and *how* it is leaving the cell. The calorimeter is instrumented in the cell chamber and in each ambidextrous leg so that temperature changes can be measured and processed into the fractional heat energy flow components. A sample of the fractional data collected during the 18650 test campaign is shown in Figure 7. The circular plots show the percentages of thermal runaway energy conducting through the cell casing, and the fractions leaving the cell top or bottom. The difference in energy flow depending on whether the cell had a bottom vent or not (at the left) and with or without bottom rupture (at the right) is apparent. From these data, it is clear that the cells tested release only a small fraction of their thermal runaway energy via conduction through the cell casing and the remaining energy is released via the vented ejecta material.

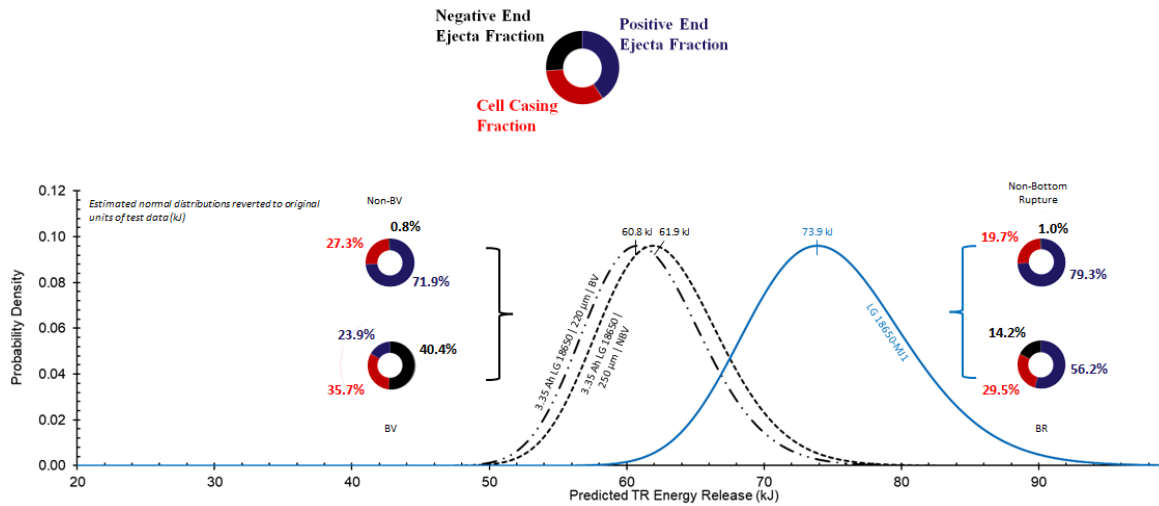


Figure 7. Comparison of energy distributions and associated energy fractions for bottom vented and non-bottom vented cells. Key at top shows: red arc represents cell casing fraction, black arc represents negative end ejecta fraction, and the purple arc represents positive end ejecta fraction. (Adapted from Ref. 13)

This thermal runaway performance observed during early S-FTRC runs has implications for battery design. Recalling that the previously mentioned 9P “picket fence” thermal analysis erroneously assumed all thermal runaway energy was transferred to the cell surface via conduction through the casing, it becomes clear that such an assumption was the likely explanation of faster propagation in the model as compared to the test. If most of the thermal runaway energy leaves a cell as vented gases and effluents as observed from early S-FTRC results, appropriate measures must be taken to accommodate this important heat transfer path into the design to prevent impingement on neighboring cells. This was incorporated into the LREBA redesign to allow for gases to vent from the battery.

S-FTRC incorporated other design features to enhance its utility. The cell chamber is made of aluminum rendering it transparent to x-rays. The calorimeter is portable and has been used in testing campaigns at synchrotron facilities in Europe where calorimetric measurements and high speed x-ray videography are performed concurrently¹⁴. Finally, exhaust gases can be captured for post-test analysis.

B. Large-format – Fractional Thermal Runaway Calorimeter (L-FTRC)

Large-format cells are finding use in aerospace and other applications. While the small-format cells such as the previously discussed 18650 show thermal runaway energies in the range of tens of kilojoules, large-format cells such as the 134 Ah cell tested release on the order of three megajoules during thermal runaway, more than an order of magnitude more than the 18650. The difference in thermal runaway energy yield between the smaller and larger cells suggests considerably more potential for a catastrophic outcome for larger cells. The insights gained from development and utilization of the S-FTRC and larger energy thermal runaway energy yield possible from large-format cells (>100 Ah) motivated the development of the L-FTRC shown in Figure 8¹⁵.

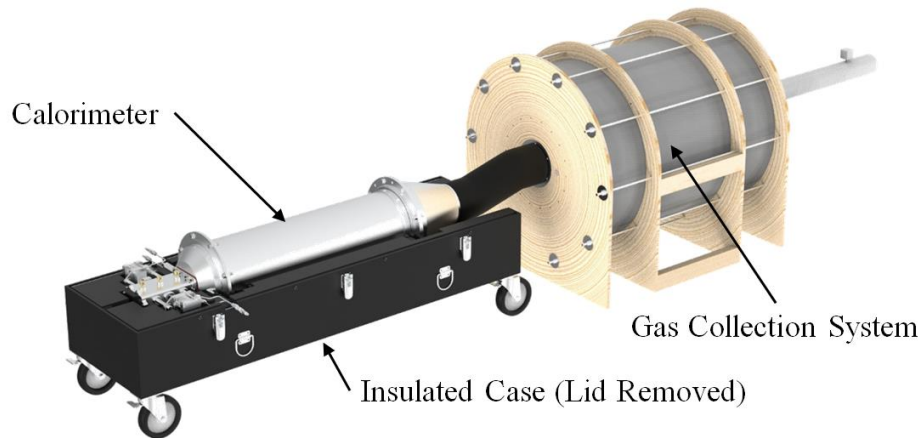


Figure 8. L-FTRC configuration showing calorimeter, insulated case (with upper lid removed), and gas collection system.

The L-FTRC internal configuration is shown in Figure 9. The operational concept for the L-FTRC is similar to that of the S-FTRC. A large-format cell is placed into a cell chamber and is set into thermal runaway using a nail penetration device. Once triggered, the cell self-heats until the cell is breached and its contents (electrode winding, ejecta, and gases) are expelled into the ejecta basket, a feature unique to the L-FTRC, which catches the ejected winding while allowing gases and ejecta to pass into a series of baffles. The expelled contents take a tortuous path through the baffle system depositing energy and soot onto the baffles before flowing through a copper mesh which removes additional energy and catches particulates for mass calculations. The entire calorimeter assembly is insulated and key components are instrumented with thermocouples to measure temperature rise. Total thermal runaway energy yield is tallied using a custom Energy Yield Algorithm (EYA) in a manner similar to that used for the S-FTRC. A number of pressure sensors are also used.

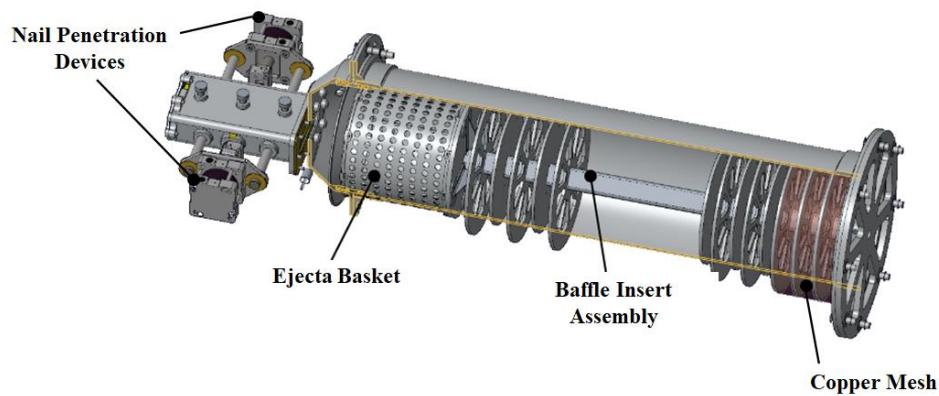


Figure 9. L-FTRC internal configuration depicting the nail penetration devices, ejecta basket, internal baffles, and copper mesh.

After leaving the calorimeter, the cooled gases flow into the gas collection system where pressure, volumetric flow rate, total volume, and gas temperature are measured. Post-test, the vent gases may be sampled for compositional analysis. Using gas volume, composition, and temperature data, the gas energy content may be determined as part of the overall thermal runaway energy tally.

During L-FTRC development, the design was refined over three iterations and once mature, a test campaign consisting of 14 live-fire runs was performed using 134 Ah GS-Yuasa cells with 100% state of charge. Thermal runaway was induced using the nail penetration system at the midpoint of each cell – approximately halfway between the terminal and the bottom end on the narrow side. The gas collection system was used successfully for a subset of these runs¹⁵.

As was done during the S-FTRC test campaign, the distribution of energy yields was determined from the measured temperature responses and EYA post-processing and is summarized in Figure 10^{16,17}. On average, the total thermal runaway energy yield was 2.86 megajoules with only 2 percent of that energy conducting through the cell casing, 53 percent contained in the ejected winding (jellyroll), and the remaining 45 percent leaving as ejecta and vented gases. To facilitate rapid test turnaround, two hardware sets were used (denoted by the red triangles and green diamonds in Figure 10). An overall probability density curve was derived based on the test results and shows the expected range of thermal runaway energies and their likelihood of occurring.

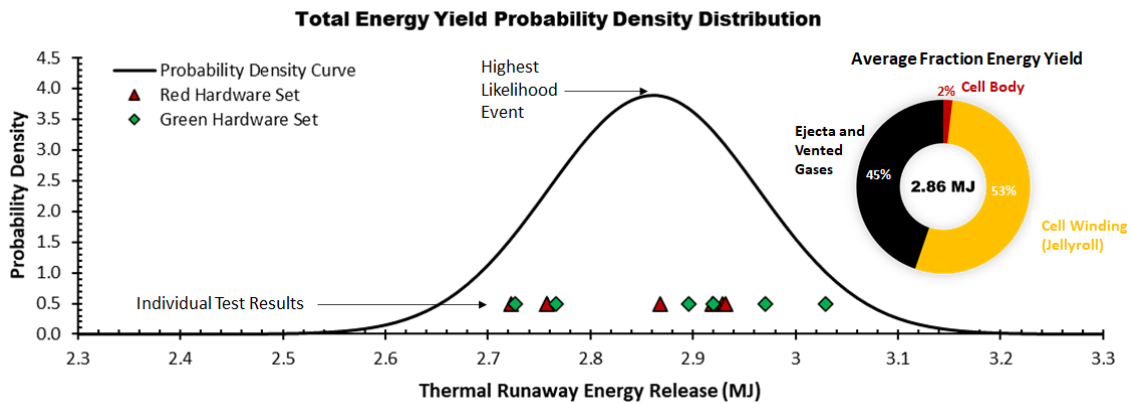


Figure 10. Total energy probability density distribution for GS Yuasa 134 Ah cell derived from test data obtained during L-FTRC testing campaign and average fractional energy yield for the cell body, cell winding (jellyroll), and ejecta and vented gases. (Adapted from Ref. 16)

Exhaust gas volume was measured by displacing air as vent gases filled a large bag in the gas collection system. A flow meter, calibrated for air, measured the air volume displaced by vent gases and was corrected once the vent gas composition was known. During the testing campaign, the gas collection system was used for a subset of the runs to collect exhaust gas samples and to measure the pressure, temperature, and volumetric flow rate of vented gases. Compositional analysis resulting from sampled gas is summarized in Figure 11^{16,17}. With known constituents, volume, and temperature, vent gas energy content may be calculated as a component of the overall thermal runaway energy yield.

Exhaust Gas Component	Run #1	Run #2	Run #3	Run #4	Run #5	Run #6	Run #7	Run #8
Carbon Dioxide, mole%	45%	<i>Insufficient Sample</i>	42%	42%	48%	41%	51%	52%
Hydrogen, mole%	35%		30%	35%	28%	33%	41%	35%
Oxygen, mole%	3%		2%	3%	1%	2%	3%	3%
Ethane, mole%	16%		15%	17%	15%	16%	2%	
Methane, mole%	1%		5%	4%			4%	
Additional HCs +/- 1%	< 1%		< 1%	< 1%	< 1%	< 1%	< 1%	
Dimethyl Carbonate, mole %	*	*	1.732%	*	1.457%	1.356%	*	1.618%
Ethyl Methyl Carbonate, mole %	*	*	5.096%	*	5.935%	7.149%	*	8.754%
Diethyl Carbonate, mole %	*	*	0.0249%	*	0.0323%	0.0394%	*	0.0511%
Total Mole% (Volume%)	100%		100%	100%	100%	100%	100%	100%

* No electrolyte data for these runs

Figure 11. Post-test compositional analysis of vent gases sampled from L-FTRC Gas Collection System.

Volumetric flow rate and pressure data are useful to understand not only how the runaway event evolves over time but also to understand run to run variability. The instantaneous exhaust gas volumetric flow rate, measured in standard liters per second (SLPS) and the expansion and collection pressures measured in the ejecta mating section and gas collection system, respectively are shown in Figure 12^{16,17}. These results demonstrate the highly variable nature of thermal runaway. The thermal runaway of Li-ion cells is violent and somewhat chaotic, so some level of variance from run to run is expected. It should be noted that Run 3 showed signs of leakage around the connection to the gas collection chamber and an elevated sustained pressure at the end of the run which suggests the bag had not been fully evacuated prior to the run. These factors help explain the lower gas volume measured for Run 3¹⁶.

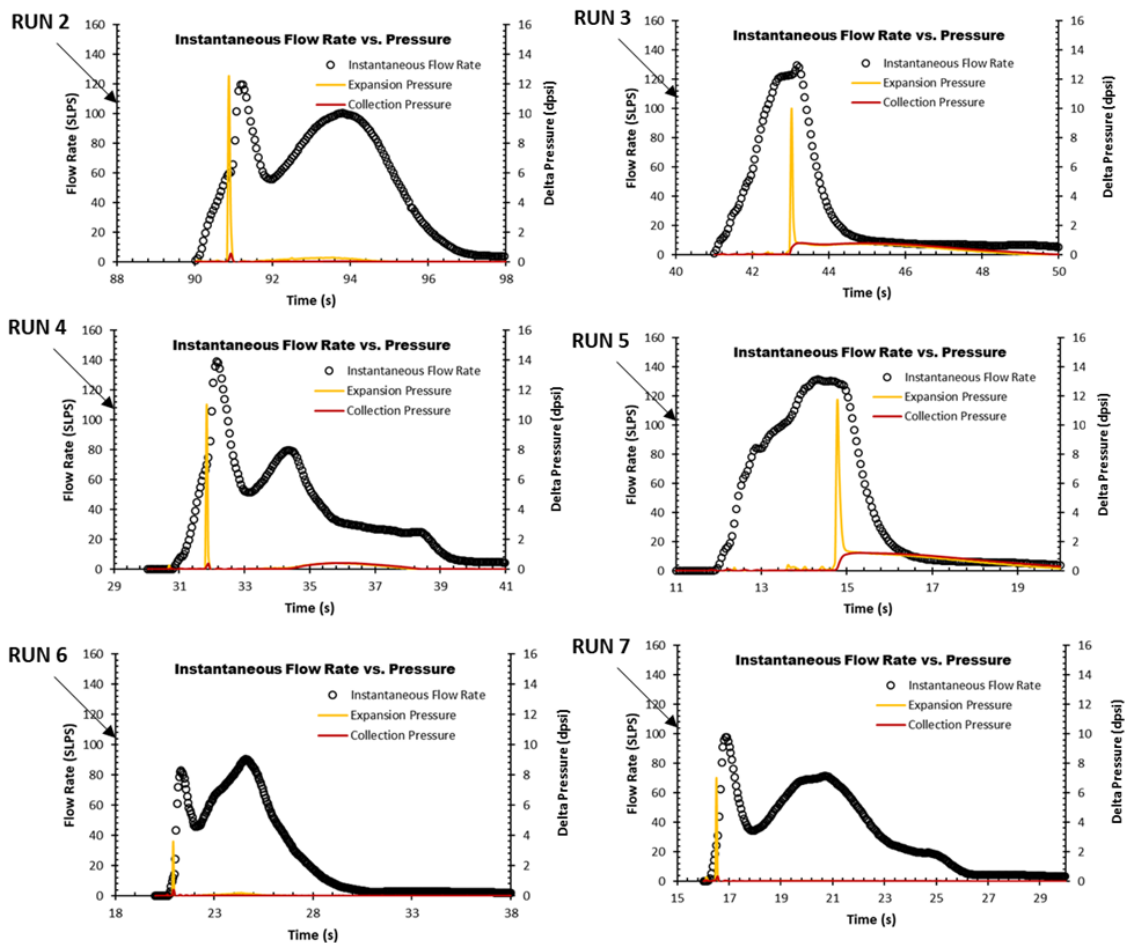


Figure 12. L-FTRC measured instantaneous vent gas volumetric flow rate and pressures measured within the ejecta mating section (expansion pressure) and within the gas collection system (collection pressure).

IV. Conclusion

Lithium-ion cells present the challenge of thermal runaway. Cell-to-cell thermal runaway propagation must be considered when designing Li-ion batteries to ensure end-user and system safety. Design and analysis require knowing not only total thermal runaway energy yield but also how the energy is distributed between that which conducts through the cell casing and that which is vented as gases and effluents. Additional benefit is gained for analysis when characterization of the total range of possible outcomes is determined (i.e. characterization of event-to-event variability and associated contributing factors). Existing calorimetric techniques provide some but not all required data. A novel NASA-developed technique, called Fractional Thermal Runaway Calorimetry, provides data to ascertain total energy yield as well as distribution amongst various heat transfer modes. FTRC allows rapid testing with fast turnaround enabling accumulation of statistically significant quantities of data.

Acknowledgments

The author thanks the S-FTRC and L-FTRC development teams composed of NASA (or former NASA): Eric Darcy, John Darst, William Walker, Damien Calderon, Richard Hagen, Ryan Brown, Barbara Sakowski, Kenneth Poast, Robert Button, Kenneth Johnson, Christopher Iannello, Erman Cihan, Peter Hughes, David Petrushenko, Sean

Comick, William Smith, Christiaan Khurana, Alex Hoffman, Hudson Mills, Eric Drake, James Thomas, Natalie Anderson, Naina Noorani, and Zoran Bilc (S&K Engineering and Research), and Gary Bayles (Science Application International Corporation).

References

- ¹Okubo, M., Ko, S., Dwibedi, D., Yamada, A., “Designing Positive Electrodes with High Energy Density for Lithium-Ion Batteries,” *J. Mater. Chem. A*, Vol. 9, 2021, pp. 7407-7421.
- ²Ifran, U., “How Lithium Ion Batteries Grounded the Dreamliner,” *Scientific American*, URL: <https://www.scientificamerican.com/article/how-lithium-ion-batteries-grounded-the-dreamliner/>, Dec. 2014
- ³Hsu, B., “Lithium Ion Batteries Ignite Three Garbage Truck Fires in California,” *Autoblog*, URL: <https://www.autoblog.com/2022/12/12/trash-truck-battery-fire-ca/>, Dec. 2022.
- ⁴Charalambous, P., “E-Bike Batteries Raise Safety Concerns Amid Rise in Fires: ‘Very Hard to Examine’,” ABC News (go.com), URL: <https://abcnews.go.com/Technology/bike-batteries-raise-safety-concerns-amid-rise-fires/story?id=95617246>, Dec. 2022.
- ⁵Hewson, J. C., Domino, S. P., “Thermal Runaway of Lithium-Ion Batteries and Hazards of Abnormal Thermal Environments,” Sandia National Laboratories, Rept. SAND2015-3080C, 9th U.S. National Combustion Meeting, Cincinnati, Ohio, May 2015.
- ⁶Ribiere, P., Grugeon, S., Morcrette, M., Boyanov, S., Laruelle, S., and Marlair, G., “Investigation on the Fire-Induced Hazards of Li-Ion Battery Cells by Fire Calorimetry,” *Energy & Environmental Science*, Vol. 5, 2012, pp. 5271–5280.
- ⁷“Aircraft Incident Report, Auxiliary Power Unit Battery Fire, Japan Airlines Boeing 787-8, JA829J,” National Transportation Safety Board, Report. NTSB/AIR-14/01, PB2014-108867, Boston, MA, Nov. 2014.
- ⁸Walker, W., Rickman, S., Darcy, E., Hughes, P., Pizano, S., Enhancing Battery Safety with Fractional Thermal Runaway Calorimetry, The Battery Show Europe 2019, Stuttgart, Germany, May 2019.
- ⁹Hatchard, T. D., MacNeil, D. D., Basu, A., and Dahn, J. R., “Thermal Model of Cylindrical and Prismatic Lithium-ion Cells,” *J. Electrochemical Society*, Vol. 148, No. 7, 2001.
- ¹⁰Rickman, S. L., Christie, R. J., White, R. E., Drolen, B. L., Navarro, M., Coman, P. T., “Considerations for the Thermal Modeling of Lithium-Ion Cells for Battery Analysis,” URL: <http://hdl.handle.net/2346/67474>, 46th International Conference on Environmental Systems, Vienna, Austria, July 2016.
- ¹¹Yathi, S., Walker, W., Doughty, D., Ardebili, H., Energy Distributions Exhibited During Thermal Runaway of Commercial Lithium Ion Batteries Used for Human Spaceflight Applications, *J. Power Sources*, Vol. 329, pp. 197-206.
- ¹²Dimpault-Darcy, E., Darst, J., Walker, W., Rickman, S., Anderson, N., Khurana, C., Drolen, B., Bayles, G., and Bilc, Z., U.S. Patent for “Systems and Methods for Measuring a Heat Response of a Battery Cell in Thermal Runaway”, No. US 11,201,358, 30 October 2018.
- ¹³Walker et al., Decoupling of heat generated from ejected and non-ejected contents of 18650-format lithium-ion cells using statistical methods, *J. Power Sources*, Vol. 415, 2019, pp. 207-218.
- ¹⁴Finegan et al., Modelling and experiments to identify high-risk failure scenarios for testing the safety of lithium-ion cells, *H. Power Sources*, Vol. 417, 2019, pp. 29-41
- ¹⁵Rickman, S. L., Fractional Thermal Runaway Calorimetry, AIChE Design Institute for Energy Relief Systems, Spring Meeting, 11 May 2022.
- ¹⁶Rickman, S.L., et al., Calorimetry for Large-format Lithium-ion Cell Thermal Runaway (TR), Volume II: GS Yuasa 134-Ah Cell Testing Summary, NESC-RP-17-01291, April 30, 2020.
- ¹⁷Walker et al., “Evaluation of Large-Format Lithium-Ion Cell Thermal Runaway Response Triggered by Nail Penetration Using Novel Fractional Thermal Runaway Calorimetry and Gas Collection Methodology,” *J. Electrochem Soc*, Vol. 169, No. 6, 2022.